

SPD-640-01

ADA 015962

HYDRODYNAMIC CHARACTERISTICS OF A CONTROL SURFACE

# NAVAL SHIP RESEARCH AND DEVELOPMENT CENTER

Bethesda, Maryland 20084



HYDRODYNAMIC CHARACTERISTICS OF A CONTROL SURFACE

by

Charles G. Moody

12

APPROVED FOR PUBLIC RELEASE; DISTRIBUTION UNLIMITED

SHIP PERFORMANCE DEPARTMENT  
DEPARTMENTAL REPORT

DDC  
RECORDED  
OCT 17 1975  
REGULATED  
B

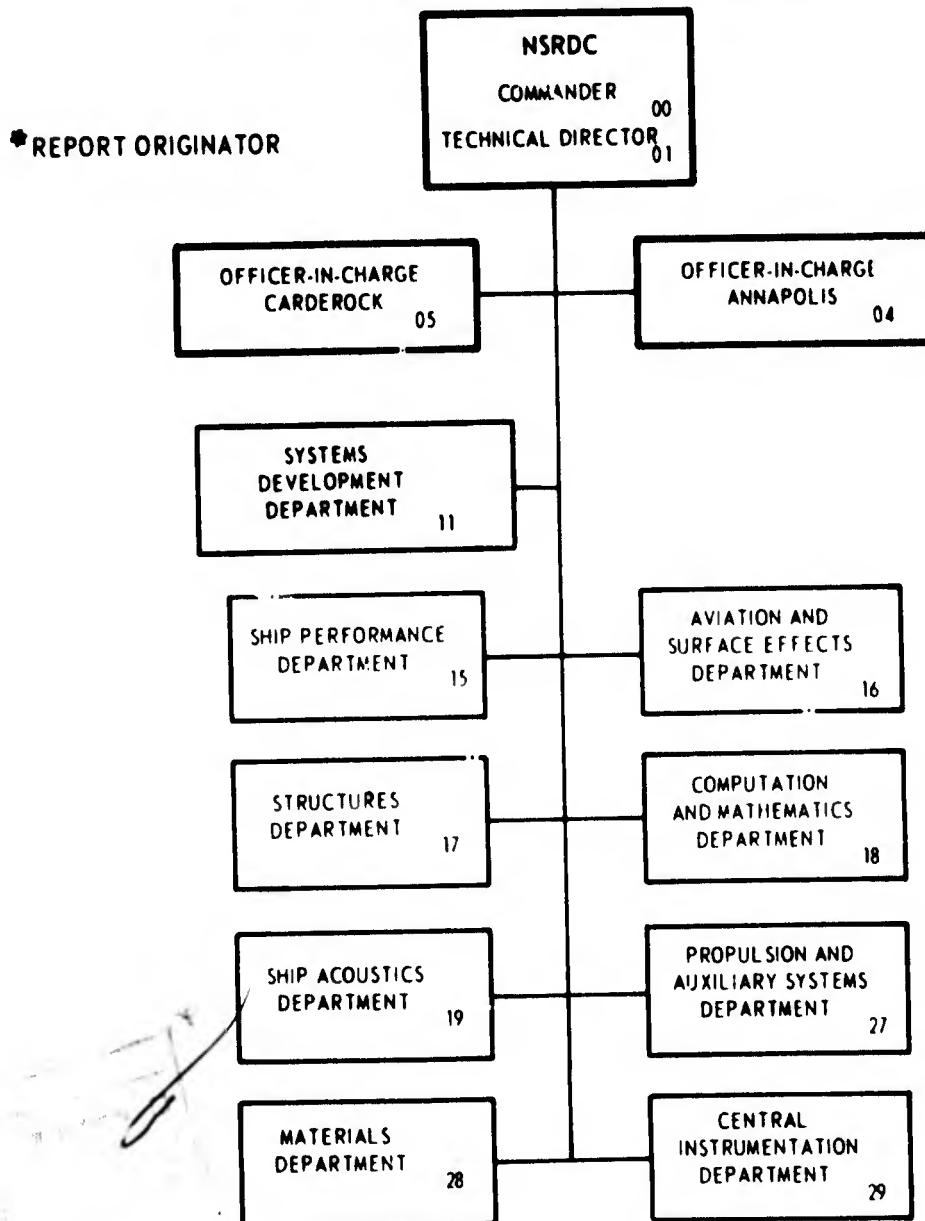
September 1975

SPD-640-01

The Naval Ship Research and Development Center is a U. S. Navy center for laboratory effort directed at achieving improved sea and air vehicles. It was formed in March 1967 by merging the David Taylor Model Basin at Carderock, Maryland with the Marine Engineering Laboratory at Annapolis, Maryland.

Naval Ship Research and Development Center  
Bethesda, Md. 20034

### MAJOR NSRDC ORGANIZATIONAL COMPONENTS

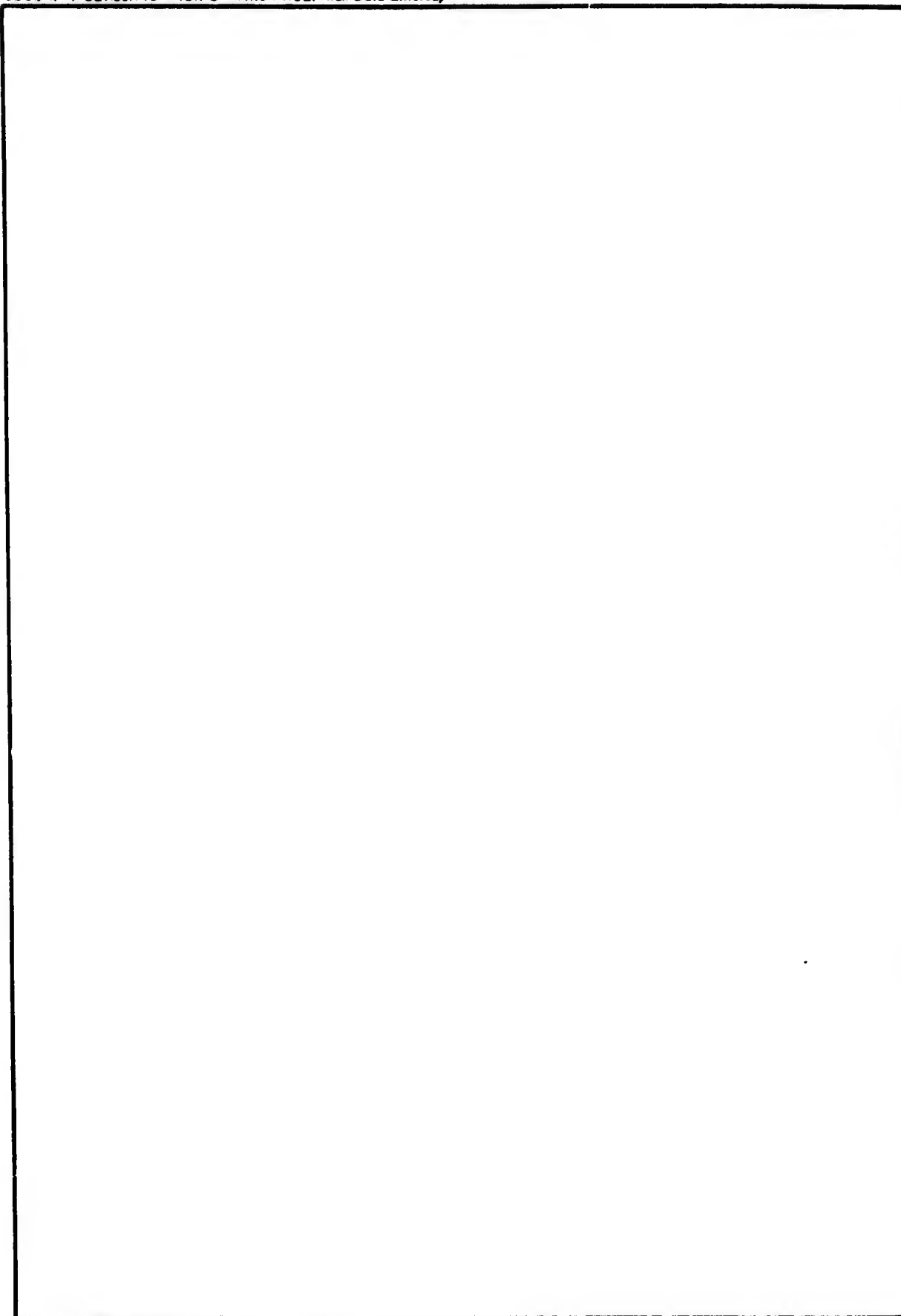


REPORT DOCUMENTATION PAGE		READ INSTRUCTIONS BEFORE COMPLETING FORM	
1. REPORT NUMBER SPD-646-01	2. GOVT ACCESSION NO.	3. RECIPIENT'S CATALOG NUMBER	
4. TITLE (and Subtitle) HYDRODYNAMIC CHARACTERISTICS OF A CONTROL SURFACE		5. TYPE OF REPORT & PERIOD COVERED Final Report	
6. AUTHOR(s) Charles G. Moody		7. PERFORMING ORGANIZATION REPORT NUMBER	
8. PERFORMING ORGANIZATION NAME AND ADDRESS David W. Taylor Naval Ship R&D Center Bethesda, Maryland 20884		9. CONTRACT OR GRANT NUMBER(s)	
10. CONTROLLING OFFICE NAME AND ADDRESS David W. Taylor Naval Ship R&D Center Bethesda, Maryland 20884		11. PROGRAM ELEMENT, PROJECT, TASK AREA & WORK UNIT NUMBERS	
12. MONITORING AGENCY NAME & ADDRESS (if different from Controlling Office)		13. SECURITY CLASS. (of this report) UNCLASSIFIED	
14. DISTRIBUTION STATEMENT (of this Report) Approved for Public Release; Distribution Unlimited		15a. DECLASSIFICATION/DOWNGRADING SCHEDULE	
16. DISTRIBUTION STATEMENT (of the abstract entered in Block 20, if different from Report)			
17. SUPPLEMENTARY NOTES			
18. KEY WORDS (Continue on reverse side if necessary and identify by block number) Rudders Cavitation Control surfaces			
19. ABSTRACT (Continue on reverse side if necessary and identify by block number) A study of the performance of a low-aspect-ratio, all-movable control surface in water is presented and compared with the performance of similar control surfaces in air. The results of this study show the free-stream characteristics of a control surface with an NACA 0015 section and a 45 percent taper ratio for different conditions affecting cavitation and stall. It is concluded that large angles of attack should be avoided under conditions that may cause stall.			

389694

13

**SECURITY CLASSIFICATION OF THIS PAGE(When Data Entered)**



**SECURITY CLASSIFICATION OF THIS PAGE(When Data Entered)**

## TABLE OF CONTENTS

	Page
ABSTRACT.....	1
ADMINISTRATIVE INFORMATION.....	1
INTRODUCTION.....	1
PROTOTYPE AND MODEL.....	3
FACILITIES AND INSTRUMENTATION.....	4
TEST PROCEDURE.....	6
TEST RESULTS.....	7
HYDRODYNAMIC AND AERODYNAMIC CHARACTERISTICS.....	13
DISCUSSION.....	16
CONCLUSIONS.....	20
RECOMMENDATIONS.....	21
REFERENCES.....	22

## LIST OF FIGURES

Figure 1 - Rudder Dynamometer.....	5
Figure 2 - Free-Stream Characteristics of Rudder M-1 for Cavitation Number 2.257 and Reynolds Number of $0.910 \times 10^6$ .....	8
Figure 3 - Free-Stream Characteristics of Rudder M-1 for Cavitation Number of 4.515 and Reynolds Number of $0.643 \times 10^6$ .....	9
Figure 4 - Free-Stream Characteristics of Rudder M-1 for Cavitation Number of 4.515 and Reynolds Number $0.910 \times 10^6$ .....	10

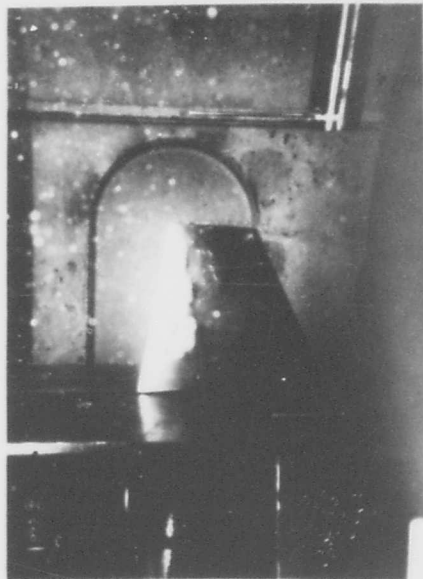
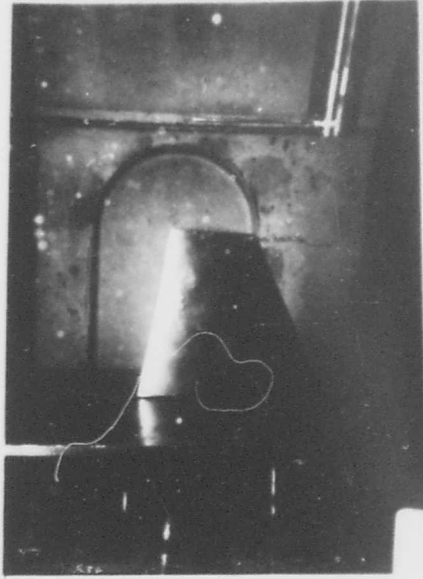
	Page
Figure 5 - Free-Stream Characteristics of Rudder M-1 with Shaft Fairing and 2-inch Clearance from Ground Board for Cavitation Number of 2.257 and Reynolds Number of $0.910 \times 10^8$ .....	11
Figure 6 - Free-Stream Characteristics of Rudder M-1 with Bare Shaft and 2-inch Clearance from Ground Board for Cavitation Number of 8.149 and Reynolds Number of $0.910 \times 10^8$ .....	12

---

Table 1 - Particulars of Model.....	4
-------------------------------------	---

## NOTATION

$C_D$	Drag coefficient $\left( \frac{\text{Drag}}{\frac{1}{2} \rho s v^2} \right)$
$C_L$	Lift coefficient $\left( \frac{\text{Lift}}{\frac{1}{2} \rho s v^2} \right)$
$\bar{c}$	Mean geometric chord
$(CP)_{\bar{c}}$	Chordwise center of pressure in percent of mean geometric chord from leading edge
$Cm_{\bar{c}/4}$	Moment coefficient about shaft at quarter-chord point of mean geometric chord
$H_s$	Static pressure head
$H_v$	Vapor pressure head
$g$	Acceleration of gravity
$Re$	Reynolds number
$\alpha$	Angle of attack
$\sigma$	Cavitation number
$\nu$	Kinematic viscosity
$\rho$	Mass density
$s$	Planform area
$v$	Velocity



## CAVITATION

Note Tip-Vortex Cavitation and Sheet Cavitation in Both Views

## ABSTRACT

A study of the performance of a low-aspect-ratio, all-movable control surface in water is presented and compared with the performance of similar control surfaces in air. The results of this study show the free-stream characteristics of a control surface with an NACA 0015 section and a 45 percent taper ratio for different conditions affecting cavitation and stall. It is concluded that large angles of attack should be avoided under conditions that may cause stall.

## ADMINISTRATIVE INFORMATION

The results of tests conducted in connection with rudder torque research are presented herein in a report sponsored by the Naval Ship Research and Development Center under General Hydromechanics Research; Project SR009 01 01, Task 00102.

## INTRODUCTION

The design of control surfaces for United States naval ships is currently based on wind-tunnel tests,<sup>1</sup> whereas the data presented herein are based on tests in water. The principal objectives of these tests are (1) to assess the effect of cavitation, which makes the conditions in water somewhat different from those in air, and (2) to study the sudden loss of lift of control surfaces at critical angles of attack. The latter is sometimes important under conditions where strong control is required.

Strong rudder action is required to control the hydrodynamic interaction forces encountered by ships in the confined waters of canals<sup>2</sup> and

---

<sup>1</sup> References are listed on page 21

during replenishment operations at sea.<sup>3</sup> This is also true of the wind and wave forces encountered in typhoons and other severe storms, and even under moderate conditions in following and oblique seas. Under all of these conditions, large rudder angles may be used to maintain a straight course, and consequently the angle of attack of the rudder is large. These conditions are quite different from those experienced in turning maneuvers where the outward movement of the stern makes the angle of attack of the rudder less than the rudder-deflection angle. The question therefore arises as to whether or not the rudder stalls at high angles of attack. If it does, the rudder becomes less effective; consequently large rudder angles should be avoided under these conditions.

For the reasons given above, the performance of rudders at large angles of attack, or incidence, is a matter of considerable interest. Moreover, the rudder torques obtained from full-scale ship trials have shown considerable scatter and tend to be larger than those obtained from model tests.<sup>4</sup> This difference between model and ship performance was one of the factors that led to the authorization of these exploratory tests.

The control surfaces of ships are subject to cavitation and free-surface effects that do not occur in air. They are also occasionally subject to high angles of attack that are not likely to occur on the control surfaces of aircraft. For instance, an airplane is turned by banking and the rudder simply helps to control the maneuver. Consequently the operating conditions for ship and aircraft control surfaces are somewhat different. There is also a difference between ship and model conditions. In model turning tests, the atmospheric pressure is not reduced to the scale of the model but is the same as for the ship. Consequently, model tests may not show the cavitation that occurs on the rudders of some ships.

One means of studying this aspect of control-surface performance is to use a variable-pressure water tunnel. Facilities of this kind have occasionally been used for rudder studies, notably at the Admiralty Experiment Works in Haslar, England. A variable-pressure rudder study is also presented in Reference 5, although in this case the data are based on visual observations without any force or moment measurements.

A difficulty in conducting rudder-cavitation studies is that air may be drawn from the surface or break through from the surface and obscure the phenomenon of cavitation. In the present tests, aeration was prevented by avoiding the use of surface-piercing apparatus and by providing an adequate head of water over the rudder.

The tests were conducted in a variable pressure water tunnel where the control surface was mounted on the bottom of the test section. The results of these tests consist essentially of basic data which are generally applicable to control surfaces such as rudders, diving planes, and roll stabilizing fins.

In this report, the hydrodynamic characteristics of a low-aspect-ratio, all-movable (spade-type) control surface are presented for different conditions affecting cavitation and stall. These characteristics are discussed with regard to their application to ship and model performance where the turbulence and Reynolds number conditions may be somewhat different from those of the tests. A comparison of these data with those in Reference 6 from wind-tunnel tests of a similar control surface is included. It is recommended that a supplementary series of tests be conducted to assess the performance of a control surface in the slipstream of a propeller.

#### PROTOTYPE AND MODEL

A low-aspect-ratio, all-movable (spade type) control surface of NACA 0015 section and 45 percent taper was the prototype for this investigation, as it was for the principal tests of Reference 6. In both cases the models represented control surfaces with turning-shaft centerlines passing through the mean chord at a point 25 percent of its length from the forward end, as shown in Figures 2 through 6. The white metal model for the water-tunnel tests had the characteristics given in the following table:

TABLE 1  
Particulars of Model M-1

Aspect Ratio	2 (with ground board)
Section	NACA 0015
Taper Ratio	0.45
Sweep Angle	0
Tip Shape	Square
Chord	7 in.
Span	7 in.
Area	0.340 sq. ft.
Shaft Location	25 percent chord

#### FACILITIES AND INSTRUMENTATION

The investigation was conducted in the NSRDC 24-inch variable pressure water tunnel where the speed and the pressure of the water in the test chamber could be adjusted to represent suitable test conditions. The rudder dynamometer was mounted on a plate in the bottom of the tunnel test chamber where it was entirely underwater during the tests. Mounting the dynamometer in this position largely eliminated the possibility of drawing air from the surface and mistaking it for cavitation.

The 24-inch variable pressure water tunnel used for this investigation is described in Reference 7. There it is referred to as a 27-inch tunnel, but the nozzle size was subsequently reduced. In these tests, it was used as an open-jet tunnel with a 24-inch nozzle. The velocity of the water in the test section was measured with a pitot tube. The test chamber was fitted with viewing windows and stroboscopic lights.

Figure 1 shows the rudder dynamometer designed for these tests. The box-shaped enclosure at the bottom of the instrument was located outside the slipstream in a recessed area of the water tunnel. The rudder and the

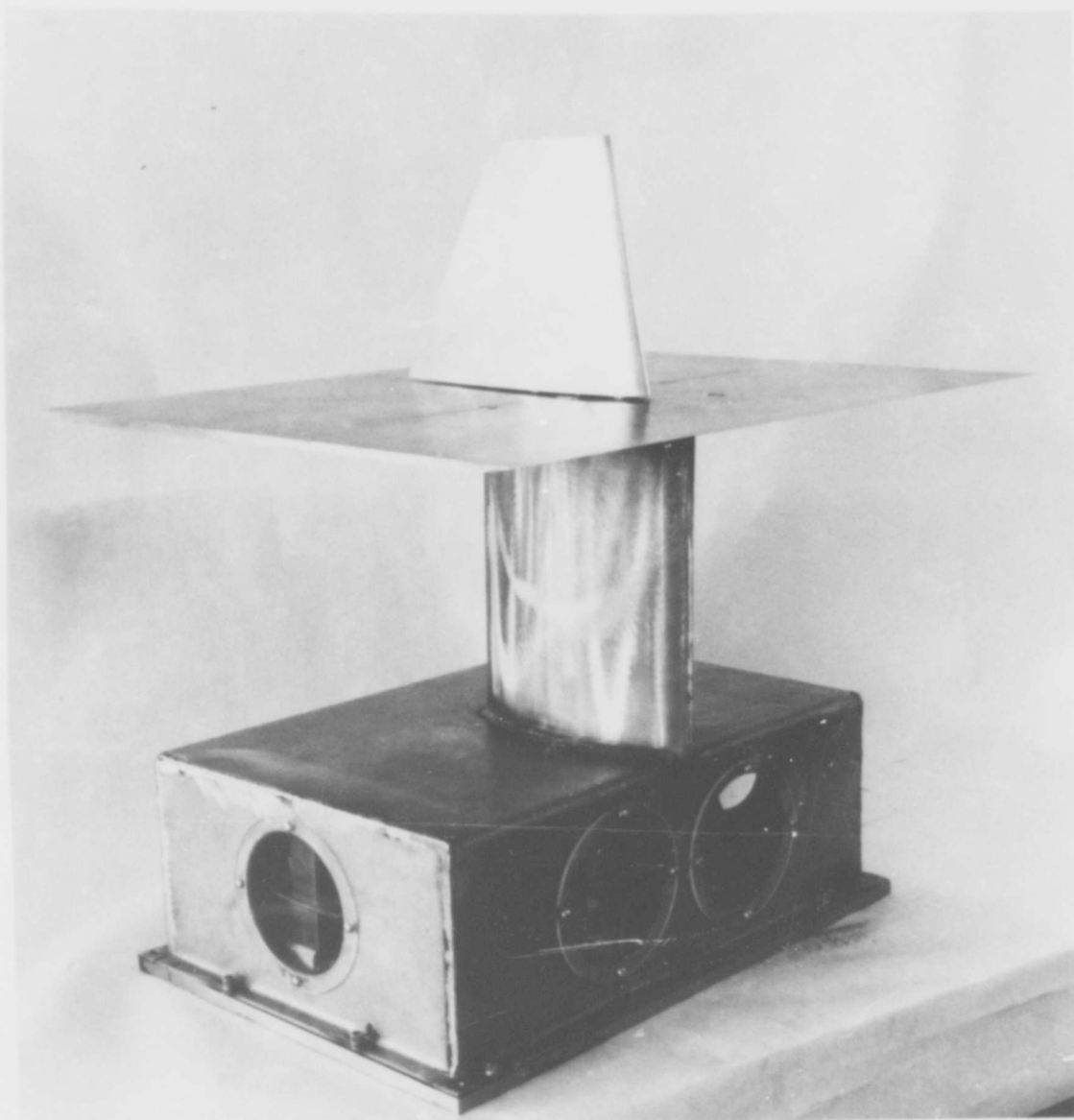


Figure 1 - Rudder Dynamometer

The dynamometer was entirely underwater in these tests. The box-shaped enclosure at the bottom of the instrument was located in a recess in the water tunnel outside the slipstream.

steel-plate ground board over which the rudder operated were in the slip-stream. The lift, the drag, and the torque of the rudder were measured by modular-force gages that were the sensing elements of the dynamometer. The force and moment data sensed by the rudder dynamometer were recorded by Brown (strip chart) recorders.

The rudder was set at the desired angle by a waterproof electric motor. The rudder angle was measured with a variable reluctance shaft-angle transducer. A digital meter was used to indicate the rudder angle.

#### TEST PROCEDURE

The tests were based on the Reynolds number

$$Re = \frac{VL}{\nu} \quad (1)$$

and on the cavitation number

$$\sigma = \frac{H_s - H_v}{V^2/2g} \quad (2)$$

These numbers are nondimensional, but in the present context where foot-pound-second units are used,

- V is the velocity in feet per second,
- L is the mean chord length of the rudder in feet,
- $\nu$  is the kinematic viscosity in feet<sup>2</sup> per second,
- $H_s$  is the static pressure head in feet of water above the center of gravity of the rudder profile area,
- $H_v$  is the vapor pressure head in feet of water, and
- g is the acceleration of gravity in feet per second<sup>2</sup>.

The Reynolds number was regulated by setting the flow velocity. The cavitation index could be simulated by adjusting either the flow velocity or the pressure; thus, in theory cavitation could be induced either by

increasing the flow velocity or by reducing the pressure. Actually, the flow velocity was limited 1) by the necessity of keeping the hydrodynamic load on the rudder within safe limits and 2) by the maximum velocity obtainable in the water tunnel. The pressure could be adjusted to suit a wide range of cavitation conditions.

### TEST RESULTS

The results of the investigation are presented in Figures 2 through 6.

Figure 2 shows the data for a cavitation number of 2.257 and a Reynolds number of  $0.910 \times 10^6$ . Under these conditions, tip cavitation occurred at a rudder angle of about 15 degrees and the rudder began to sing. Tip and nose cavitation occurred at an angle of about 20 degrees and the rate at which the lift increases with rudder angle began to decline. Tip, nose, and flashes of face cavitation occurred on the low-pressure or suction side at a rudder angle of 25 degrees. Flow breakdown occurred at about 25.4 degrees. At 32 degrees there was tip cavitation only, and at 35 degrees there was no visible cavitation.

Figure 3 gives the data for a cavitation number of 4.515 and a Reynolds number of  $0.643 \times 10^6$ . Under these conditions the rudder lift increased steadily without any significant reduction due to cavitation until flow breakdown occurred at an angle of about 27 degrees.

Figure 4 gives the data for a cavitation number of 4.515 and a Reynolds number of  $0.910 \times 10^6$ . The rate of lift increase with rudder angle began to decline at about 22 degrees where cavitation became significant, and breakdown of flow occurred at about 27 degrees.

Figure 5 presents the data for a cavitation number of 2.257 and a Reynolds number of  $0.910 \times 10^6$  with a 2-inch fairing around the rudder shaft between rudder and the baseplate. The lift coefficient shown in this figure for the rudder with the fairing is more favorable than that

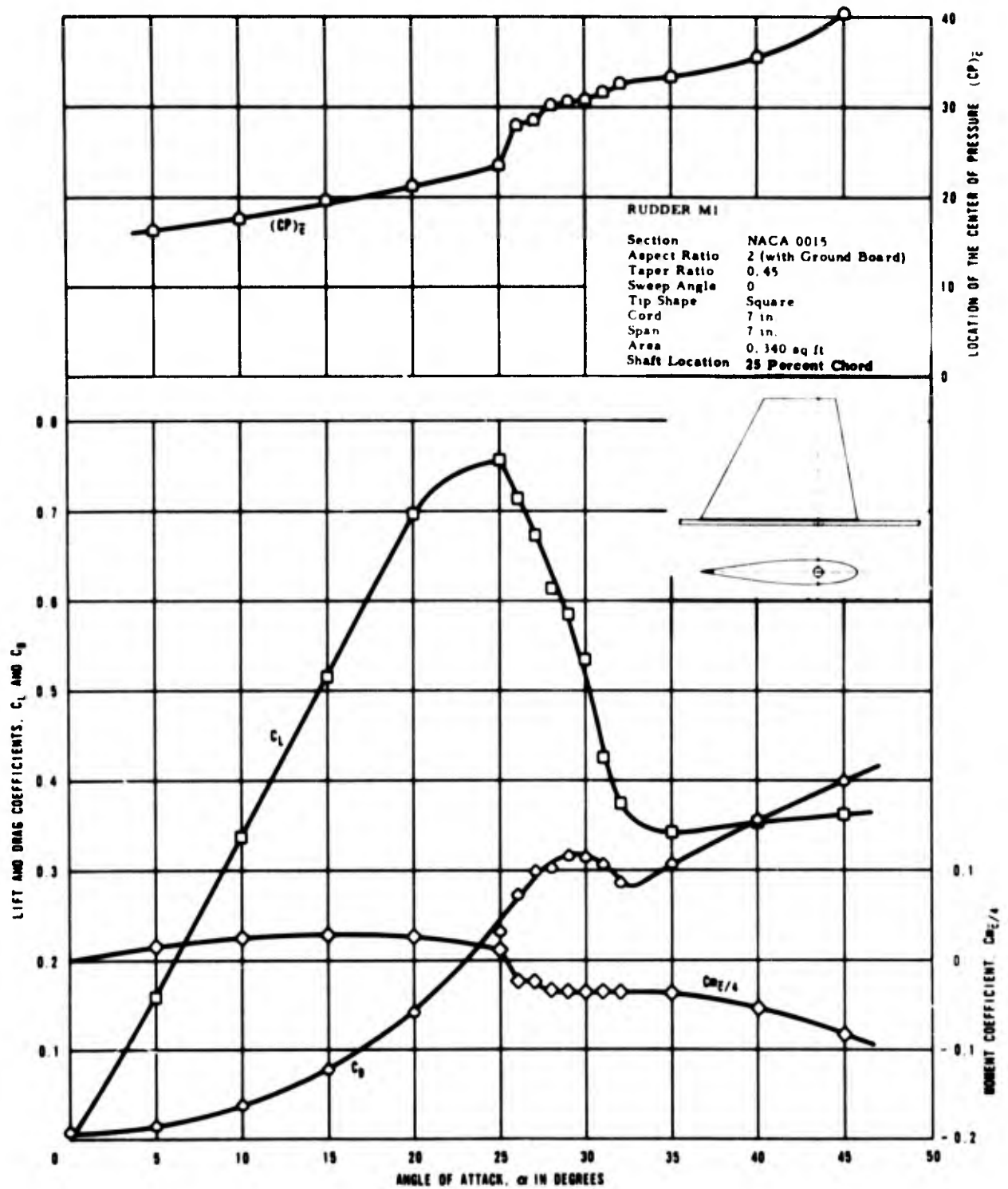


Figure 2 - Free-Stream Characteristics of Rudder M-1 for Cavitation Number 2.257 and Reynolds Number of  $0.910 \times 10^6$

Speed, 10 knots. Head, 10 feet (absolute-vapor).

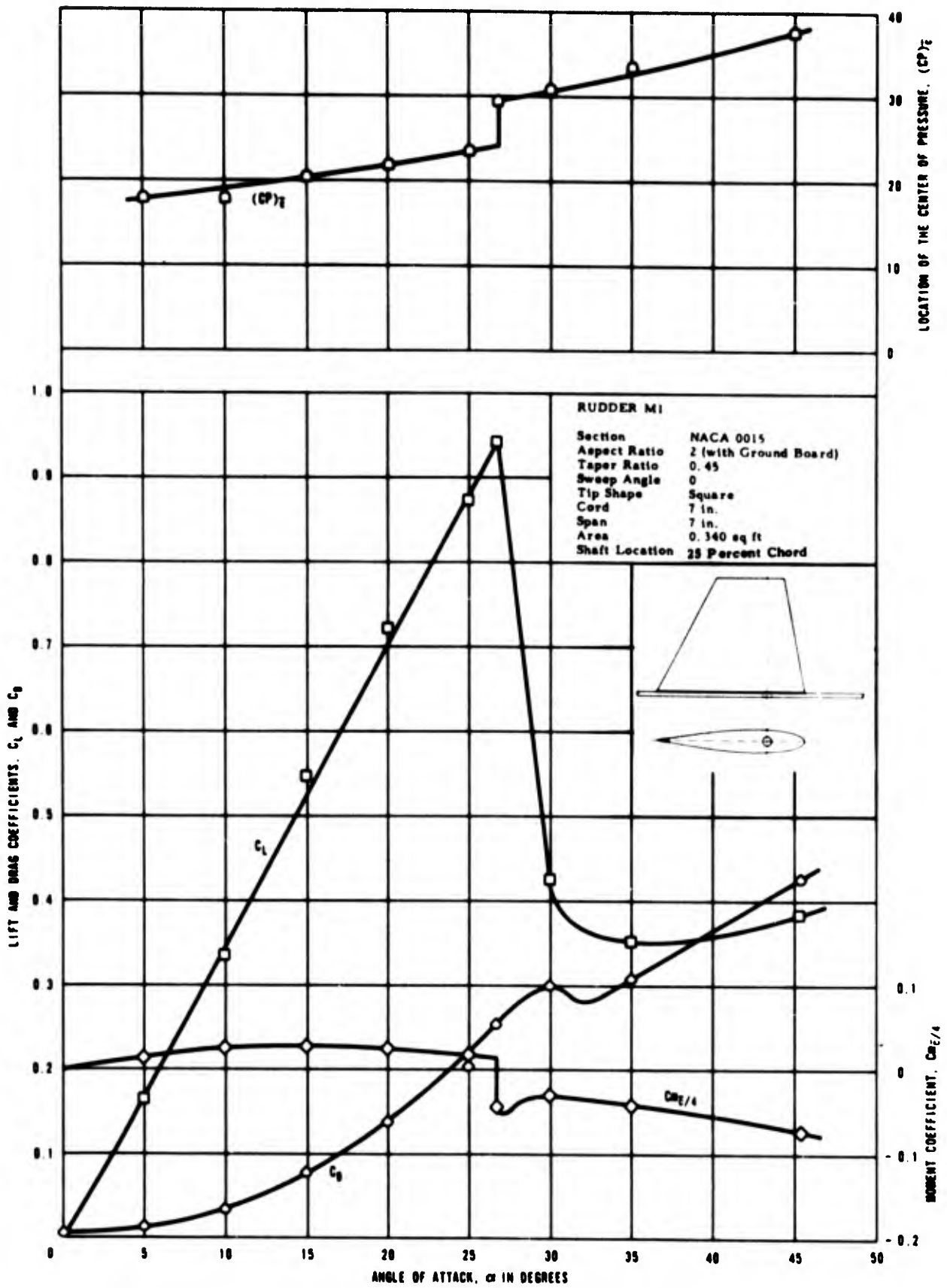


Figure 3 - Free-Stream Characteristics of Rudder M-1 for Cavitation Number of 4.515 and Reynolds Number of  $0.643 \times 10^8$

Speed, 7.0711 knots. Head, 10 feet (absolute-vapor).

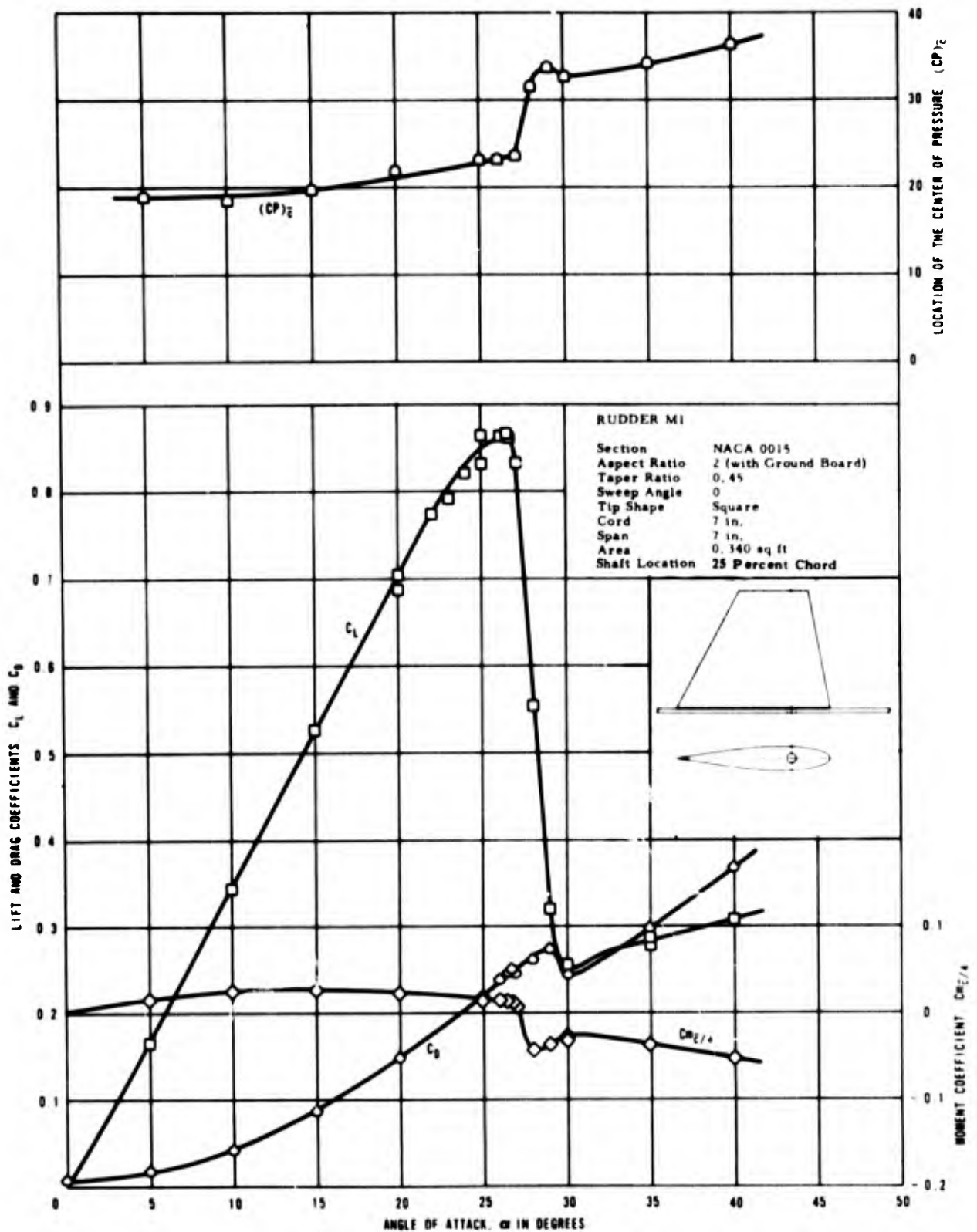


Figure 4 - Free-Stream Characteristics of Rudder M-1 for Cavitation Number of 4.515 and Reynolds Number  $0.910 \times 10^6$

Speed, 10 knots. Head, 20 feet (absolute-vapor).

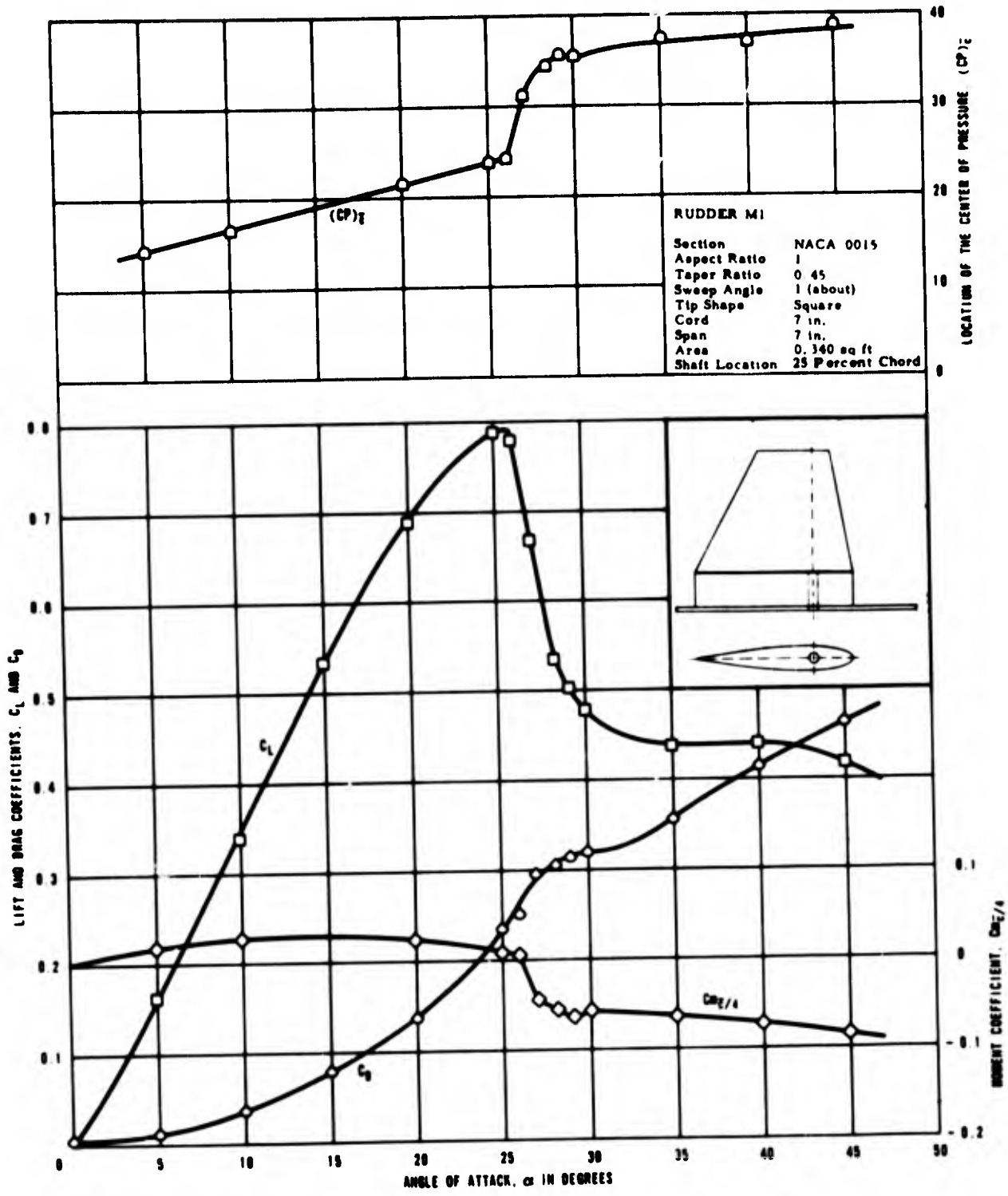


Figure 5 - Free-Stream Characteristics of Rudder M-1 with Shaft Fairing and 2-inch Clearance from Ground Board for Cavitation Number of 2.257 and Reynolds Number of  $0.910 \times 10^8$

Speed, 10 knots. Head, 10 feet (absolute-vapor).

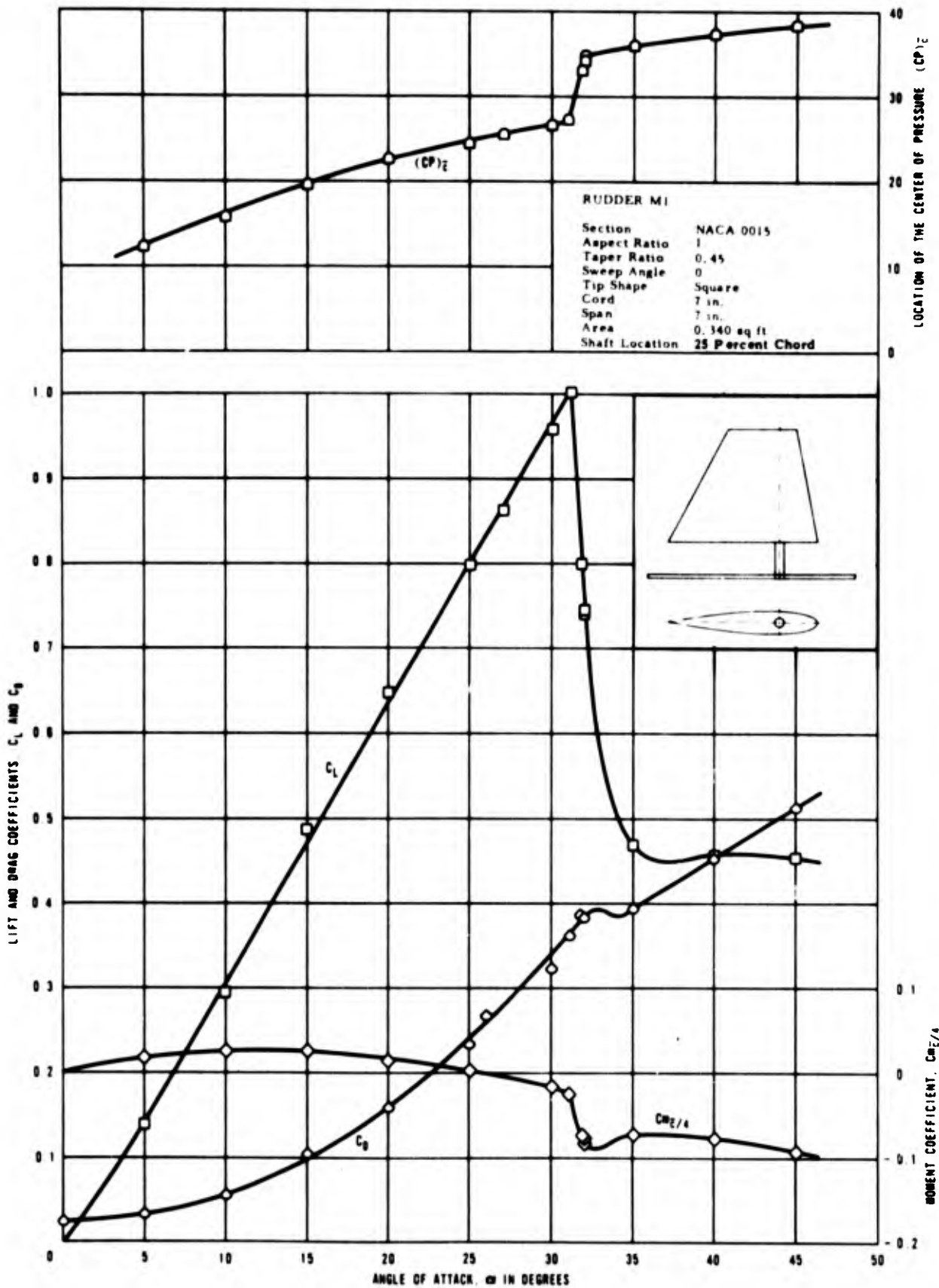


Figure 6 - Free-Stream Characteristics of Rudder M-1 with Bare Shaft and 2-inch Clearance from Ground Board for Cavitation Number of 8.149 and Reynolds Number of  $0.910 \times 10^6$

Speed, 10 knots. Head, 36.1 feet (absolute-vapor).

shown in Figure 2 for the rudder without the fairing, and breakdown occurred at a slightly larger angle of attack. Cavitation was profuse.

Figure 6 shows the data for a cavitation number of 8.149 and a Reynolds number of  $0.910 \times 10^6$  with a 2-inch space between the rudder and the base-plate. Under these conditions, with no cavitation effect, the lift increased steadily until breakdown of the flow occurred at a rudder angle of about 31 degrees.

The maximum lift coefficient shown in Figure 2 is about 0.75. As Figure 3 indicates, this coefficient can be increased by reducing the speed and thus increasing the cavitation number, while also reducing the Reynolds number. Figure 4 shows that it can also be increased without reducing the Reynolds number by increasing the pressure head. A maximum lift coefficient of about 0.86 can then be obtained, which is about 15 percent more than that shown in Figure 2.

Figure 5 indicates that the rudder performance may be improved somewhat by the addition of a fixed streamlined fairing between the rudder and the hull of the ship. Comparison with Figure 2 shows that the maximum lift is increased about 5 percent and that the lift after breakdown at a rudder angle of 35 degrees is increased about 28 percent. The atmospheric pressure conditions represented in Figure 6 apply to model tests. Under the high pressure of the model conditions and with the rudder 2 inches clear of the plane surface, flow breakdown did not occur until the rudder angle was about 31 degrees. In Figure 6, the resistance of the exposed part of the rudder shaft is included in the drag coefficient.

#### HYDRODYNAMIC AND AERODYNAMIC CHARACTERISTICS

Hydrodynamics and aerodynamics are divisions of the basic science of fluid dynamics. Basic data can therefore be obtained from tests in water or air with equal validity as long as consideration is given to free-surface effects and to such factors as the difference in the compressibility of

the fluids, and in the effects of temperature on their kinematic viscosities. Hence it is not surprising that the results of the water-tunnel and wind-tunnel tests are in good agreement except where such factors make a difference. As might be expected, the principal difference results from the fact that cavitation does not occur in wind-tunnel tests.

The data from these water-tunnel tests can be compared with those from wind-tunnel tests of control surfaces in Reference 6. The rudder angle at breakdown and the center of pressure location are much the same in the data from both sources, but the water-tunnel tests gave a smaller lift coefficient. This may be because the flat plate over which the rudder was mounted in the water-tunnel was not quite large enough. Consequently, the effective aspect ratio of the rudder in these tests may be somewhat less than 2, but in the wind-tunnel tests where the rudder has a large plane surface, or ground board, immediately under it, the effective aspect ratio is 2. In open flow without any ground board or boundary condition, the rudder has an effective aspect ratio of 1.\* In this connection, it may be of interest to note that for an angle of attack of 20 degrees the wind-tunnel data in Figures 51 and 40 of Reference 6 give lift coefficients of 0.865 and 0.570 for aspect ratios of 2 and 1 respectively, whereas in the water-tunnel data the lift coefficient is 0.700. Therefore, the effective aspect ratio appears to be less than the nominal value of 2.

A reasonable assumption, considering the operating conditions, is that the flow in the water-tunnel tests was more turbulent than the flow in the wind-tunnel tests. Consequently, the best comparison with the data presented herein is probably afforded by wind-tunnel data for a slightly higher Reynolds number. For example, in comparing the data in Figure 4 of this report with the data from the wind-tunnel tests, it may be better to use Figure 52 of Reference 6 where the Reynolds number is  $1.40 \times 10^6$  rather than Figure 51 of that reference where the Reynolds number is  $0.931 \times 10^6$ .

---

\* There is also a difference between the down-draft effect of an open jet tunnel and the up-draft effect of a closed jet tunnel.<sup>8</sup> In rudder tests this difference may be appreciable.

As Reference 5 shows, the wind-tunnel tests were stopped at the point where breakdown occurred. Vibration may have been excessive beyond that point. However, the water-tunnel tests were carried further because they clearly showed some characteristics of interest in shiphandling. For instance, that the lift coefficient after breakdown is larger when there is a gap between the rudder and the hull, as shown in Figure 6. Since the center of pressure is further aft and the moment larger, however, the strain on the steering gear would be greater. It is of interest to note in this connection that the full-rudder angle on most ocean ships is about 35 degrees.

The data presented show that the breakdown of lift is followed by a brief lag after which the drag coefficient tends to decrease. This is shown in the curves by hollows that usually appear just before the point where the maximum reduction in lift occurs. According to Reference 9, "airfoils of aspect ratio of approximately 1.5 and smaller show a sharp decrease of drag coefficient immediately after passing the burble point." The data in Reference 6 for control surfaces with NACA 0015 section indicate an increase in drag coefficient after breakdown, but the plots do not extend far enough to show fully what does happen. This reference shows a reduction in drag after breakdown at low Reynolds numbers for control surfaces in the astern condition and for those of TMB 07507515 section shape in the ahead condition. Since the decrease in drag in the water-tunnel data presented herein is for low Reynolds numbers, the rudders of ships at higher Reynolds numbers might not be expected to exhibit this tendency. However, the full-scale rudder data in Reference 4 shows a reduction in drag after breakdown.

From a comparison of the conditions in Reference 4 with those of the water-tunnel tests in Figure 2, it is obvious that the rudder of the ship, the USS NORFOLK (DL-1), was cavitating when breakdown occurred. This may be one reason why the rudder torque of the ship was relatively greater than that of the model.

Although the characteristics of poorly shaped control surfaces may change radically with Reynolds number, those of well shaped control surfaces do not seem to change greatly except that their range of performance is extended at higher Reynolds numbers. Thus, in comparing the data in Figure 51 of Reference 6 for a Reynolds number of  $0.931 \times 10^6$  with those in Figure 55 for a Reynolds number of  $2.72 \times 10^6$ , we find that the lift and drag coefficients are a little larger at the higher Reynolds number but the principal difference is that the breakdown point is changed from an angle of 23.6 degrees at the lower Reynolds number to 28.7 degrees at the higher Reynolds number. The corresponding change in the maximum rudder torque is from -0.05 to -0.085, an increase of 70 percent. The effect of Reynolds number on the angle at which breakdown occurs may be another reason why the maximum rudder torque of the ship is relatively greater than that of the model.

#### DISCUSSION

Data from water-tunnel tests at higher Reynolds number would be of basic interest. As Equation (1) shows, higher Reynolds numbers can be obtained without changing the kinematic viscosity by increasing either the velocity of flow or the linear size of the model. For geometrically similar rudders, the Reynolds number is proportional to the force; so as far as the load on the dynamometer is concerned, it does not matter in the least whether the velocity or the size is increased. However, the stress in the rudder stock varies as the square of the speed but does not change with size. For this reason and because the range of smooth-flow velocities is limited, the use of small models is somewhat restricted.

In the large (36-inch) NSRDC water-tunnel it should be possible with suitable models to obtain a range of Reynolds numbers equal to that represented in Reference 6. Such tests definitely would be of value in

providing background information and a full understanding of the subject. Attention is called, however, to the possibility of obtaining better results from model tests of control surfaces without resorting to higher Reynolds numbers by increasing the turbulence in the flow.<sup>10</sup>

In the example worked out in Appendix A of Reference 1, a Reynolds number of  $34 \times 10^6$  was obtained for the rudder of a ship at a speed of 30 knots. This is far beyond the scope of any wind-tunnel or water-tunnel data that are presently available. Some assurance can be derived from the fact that the characteristics of low-aspect ratio control surfaces with NACA 0015 sections tend to stabilize at Reynolds numbers within the scope of existing data. Yet there are numerous full-scale effects that remain subject to conjecture.

The data presented are for control surfaces in free-stream flow. In the wake of a ship or of a ship model the turbulence is increased by the flow over the length of the hull so that the conditions are somewhat different from those in free-stream flow. In the slipstream of a propeller, both the turbulence and the flow velocity are increased and the angle of incidence varies over the leading edge of a control surface. These conditions have the effect of an increased Reynolds number. Control surfaces therefore tend to stall at larger angles of incidence in the wake of a ship or model than in free-stream flow. Moreover, at large deflection angles in the slipstream of a propeller, the forces on a control surface may not be due to lifting action but rather to deflection of the slipstream. For instance when a ship is maneuvering without appreciable headway, the action of the propeller slipstream on the rudder is much the same as that of a jet impinging on a plane surface. The slipstream of a propeller also has a significant effect on the pressure distribution and on the torque of a control surface at high speeds.

Under conditions that do not cause stall, a large part of the lift force on a control surface is due to the reduction of pressure on the suction side.<sup>11</sup> In water, the pressure on a control surface can be reduced

to the vapor pressure, which is 0.25 psi for distilled water at a temperature of 15 deg C. When water contains air, which it usually does, the minimum pressure is the combined vapor and gas (air) pressure. Where aeration occurs, air is drawn from the surface at atmospheric pressure, which is 14.7 psi under standard conditions. This, of course, can have a drastic effect.

Where cavitation occurs on a control surface, the pressure is reduced to that of the combined vapor and gas pressure which varies with temperature and air content but is otherwise stable.<sup>12</sup> Consequently, no further reduction in pressure is likely although the size of the low-pressure area may change with speed and angle of attack. In the data presented, the slope of the lift curve begins to decrease at the point where cavitation becomes significant. Cavitation can cause a large reduction in lift, but the reduction is usually gradual rather than a sudden stall.<sup>13</sup> It can also affect the virtual shape of a control surface by changing the contour around which the streamline flow occurs. Thus, it can affect the angle at which a control surface stalls. It is conceivable that the addition of the cavity shape to the control surface shape may in some instances increase the angle of stall.

When the difference between the cavitation pressure and the atmospheric pressure is sufficient to cause air to break through from the surface, the air fills not only the cavity but also the surrounding space where the pressure is less than atmospheric. Aeration can cause stall under conditions where cavitation does not even exist. Therefore, surface-piercing appendages and other sources of aeration should be avoided.

Cavitation is more likely to occur on ships than on models since the atmospheric pressure is effectively smaller under full-scale conditions. The data presented in Figure 2 for a control surface under reduced-pressure conditions show breakdown at an angle of attack of 25 deg. This is barely adequate according to Reference 1, which assumes that the maximum angle of attack on the rudder of a turning ship is 5/7 of the rudder-deflection angle. However, on a full-scale ship where a rudder operates at a higher

Reynolds number and in a turbulent wake, breakdown may be expected to occur at a larger angle of attack than in the tests. Consequently, the data presented are reassuring as far as turning maneuvers are concerned.

There is no such assurance that the rudder of a ship will not stall before reaching an angle of attack of 35 deg. Contrary to cavitation, stall is less likely to occur on ships than on models since the Reynolds number is larger under full-scale conditions. The effect of Reynolds number on stall is not well established for these conditions, but it could be assessed in laboratory tests. Tests could also be run on a ship with multiple rudders controlled independently. The angle at which breakdown occurred could be determined by putting strain gages on the rudders and turning them in opposite directions during high-speed tests. Indeed, it would seem perfectly possible to determine the angle at which stall occurs from the point at which the torque and the ram pressure of the steering gear are reversed or--in the case of control surfaces of low-aspect ratio--show a sudden change. Such tests would be of considerable interest. At present we can only conclude that large angles of incidence should be avoided under conditions in which breakdown is harmful.

Notwithstanding the paucity of conditions represented in this investigation, the results show that cavitation can be a significant factor in the performance of control surfaces at high speeds. On a fast merchant ship such as a modern container ship with a speed of over 30 knots the rudder-cavitation index may be less than half the minimum value simulated in these tests. Consequently the cavitation may be even more severe than that observed in the water-tunnel.

As previously noted, stall will generally occur at larger angles of incidence on full-scale control surfaces than in model tests as the increased Reynolds number and turbulence will augment the momentum of the fluid in the boundary layer of the surface. In some instances this may be sufficient to prevent stall at all angles of incidence over the operating range of the control surface; in others it may not be sufficient. The effect of high Reynolds-number conditions is the principal factor affecting the performance of control surfaces that remains to be assessed.

## CONCLUSIONS

For all-movable control surfaces such as rudders, diving planes, and stabilizing fins, it is concluded that cavitation 1) may limit the possible lift, and 2) may affect the angle at which flow breakdown occurs. Thus, cavitation reduces the effectiveness of a control surface.

Cavitation can cause a significant reduction in lift, but usually causes a gradual reduction rather than a sudden stall. According to these tests, its effect is by no means as drastic as flow breakdown, although it can cause breakdown by its effect on the streamline flow. In extreme instances, or where it is accompanied by aeration, cavitation can have a major effect.

## RECOMMENDATIONS

The following conclusions and suggestions are presented as recommendations:

1. In the handling of ships, the rudder should be controlled so that large angles of incidence will be avoided under conditions that may cause stall.
2. The scope of this investigation should be extended to represent lower cavitation numbers and higher Reynolds numbers.
3. A supplementary series of tests should be conducted to assess the performance of a control surface in the turbulent slipstream of a propeller.

## REFERENCES

1. Taplin, A., "Notes on Rudder Design Practice," Presented at First Symposium on Ships Maneuverability, 24-25 May 1960, pp. 127-149, David Taylor Model Basin Report 1461 (Oct 1960).
2. Moody, C. G., "The Handling of Ships through a Widened and Asymmetrically deepened Section of Gaillard Cut in the Panama Canal," David Taylor Model Basin Report 1705 (August 1964).
3. Moody, C. G., "The Interaction Effect of a Large Aircraft Carrier on a 770-foot Fast Combat Support Ship (AOE) During High-Speed Replenishment Operations," David Taylor Model Basin C-1267 (July 1961).
4. Becker, L. A. and Brock, J. S., "The Experimental Determination of Rudder Forces During Trials of USS NORFOLK," Transactions of the Society of Naval Architects and Marine Engineers, Vol. 66, pp. 310-344 (1958).
5. Hagen, G. R., "Lift, Drag, and Cavitation Characteristics of Two Proposed Rudders for the DD927 Class," David Taylor Model Basin Report C-207 (March 1949).
6. Whicker, L. F. and Fehlner, L. F., "Free-Stream Characteristics of a Family of Low-Aspect-Ratio, All-Movable Control Surfaces for Application to Ship Design," David Taylor Model Basin Report 933 (December 1958).
7. Mumma, F. G., "The Variable-Pressure Water Tunnels at the David W. Taylor Model Basin," Transactions of the Society of Naval Architects and Marine Engineers, Vol. 49, pp. 57-61 (1941).
8. Diehl, W. S., "Engineering Aerodynamics" (Revised Edition), p. 83, The Ronald Press Company, New York (1936).
9. Zimmerman, C. H., "Characteristics of Clark Y Airfoils of Small Aspect Ratio," National Advisory Committee for Aeronautics Report No. 431 (1932).

10. Goldstein, S., "Modern Developments in Fluid Dynamics, Oxford University Press (1938).
11. Lotveit, M., "A Study of Rudder Action with Special Reference to Single-Screw Ships," Transactions of the North East Coast Institution of Engineers and Shipbuilders, Vol. 75, pp. 87-124 (1959).
12. Ripken, J. H. and Killen, J. M., "Gas Bubbles: Their Occurrence, Measurement, and Influence in Cavitation Testing," Presented at IAHR Symposium on Cavitation and Hydraulic Machinery, Sendai, Japan (Sep 1962).
13. Mandel, P., "Some Hydrodynamic Aspects of Appendage Design," Transactions of the Society of Naval Architects and Marine Engineers, Vol. 61, pp. 464-515 (1953).

## INITIAL DISTRIBUTION

### Copies

- 1 CNO
  - 1 Surface Warfare Div (NOP-32)
  
- 3 NAVSEASYSKOM
  - 1 Materials and Mechanics Div (SEA 035)
  - 1 Mechanics Branch (SEA 0351)
  - 1 Advanced Ship Development Branch (SEA 03)
  
- 6 NAVSEC
  - 1 Technical Library (NSEC-6034)
  - 1 Design Branch (NSEC-6113)
  - 1 Advanced Technology Branch (NSEC 6114)
  - 1 Hull Form & Fluid Dynamics (NSEC-6136)
  - 1 Ship Performance & Trial Section (NSEC-6144G)
  - 1 Ship Control Sys Equipment Branch (NSEC-6165)
  
- 1 NAVFAC
  - 1 Consultant Waterfront Structures (NFAC-04B5)
  
- 1 ADMIN, MARAD
  - 1 Div of Ship Design